Developing local scour equations for piers with side slopes

Kasem S. El- Alfy, Mohamed T. Shamaa & Haider H. Al-tameemi

Abstract— Along a river, local scour can causes bridge collapse. Therefore, several investigations have been performed to find the best pier shape as a local scour countermeasure. Also, developing equations to forecast the depths of local scour around piers is important for safe design of bridge piers' foundation. As a result, developing pier scour equations is the main goal of this paper. Those equations are related to piers has side slope namely, semi-conical piers and semi-conical piers with upstream curved face. As well, the type of relationship between the dependent parameter (the normalized scour depth) and independent parameters (Froude number, flow intensity, angle of side slope and normalized Arc height) of developed equations in this paper is clarified.

Key words: Bridges, side slope, scour depth, semi-conical pier.

1 Introduction

CONSTRUCTION of bridges along a river leads to local scour. Local scour is the removal of bed material around an obstacle submerged in flow field. The local scour can cause a number of problems because it works to locally modify the river's equilibrium. The possible undermine of piers foundations due to local scour represents the biggest danger. This type of scour can cause bridge collapse. If disaster of bridge collapse occurs, the prices related to human life in addition to economic resources are often very high [2].

A shape of bridge piers has a significant influence on local scour [2]. Therefore, several investigations have been performed to find the best pier shape as a local scour countermeasure. For example, Mostafa (1994), cited in [12], has measured the depths of local scour for a variety of different pier shapes. Pier shapes in his study have identical projected width. His results have shown that the least scour is achieved by using the circular pier. Also, the scour depth achieved by an aero foil shape of bridge pier is less than its counterpart resulted by the circular pier [6], [3]. Furthermore, the scour depth caused by position of bridge pier according to flow direction is less than its counterpart related to circular pier [2]. Finally, the semi-conical pier produces scour depth less than its counterpart related to the vertical cylindrical pier [9].

The accuracy of maximum scour depth at bridges is very important for safe design of their foundation [14]. Developing equations, which based on a multiple regression analyses, is useful to forecast the depths of local scour around piers [15].

In this paper, the main objective is to develop empirical equations to forecast the maximum scour depth around piers with side slope which referred to as semi-conical piers and semi-conical piers with curved face. In addition, the type of relationship between the dependent and independent parameters of developed equations is illustrated.

- *Kasem S. El- Alfy, Prof. of Hydraulics, Mansoura University, Dean of Mansoura High Institute of Eng. And Technology.*
- *Mohamed T. Shamaa, Associ. Prof. of Hydraulics, Mansoura University, Irrigation and Hydraulics Dept.*
- *Haider H. Al-tameemi, P.h.D. Student, Mansoura University, Irrigation and Hydraulics Dept.*

2 Literature Review

Piers with side slope are denoted as semi-conical or conical piers (cone shaped piers). In relative to existent studies, there are differences in depths of scour around cone shaped piers compared with their counterparts of cylinders. According to [8], the local scour around the circular shaped pier and conical shaped piers with different side slopes has been assessed. The local scour as well has been assessed with the same aforementioned piers but these piers are with slot. All experiments with the test duration of 8 hours have been run at conditions of clear water and steady flow by using uniform sediment (sand). They have pointed out that the scour depth and volume around conical shaped piers with or without slot are reduced in relative to their counterparts around the circular shaped pie with or without slot.

As mentioned by [16], an experimental study has been performed to investigate the scour development around semi-conical piers and illustrate the impact of their side slopes on scour depth. All experiments have been performed on elliptical and circular piers with different side slope angles under the condition of steady flow, clear water and test duration of 24 h. The results have revealed that pier with small side slopes can even reduce the depth of scour at upstream and downstream side of pier. Moreover, the depths of scour, related to the pier with largest angle of side slop and with circular section, are decreased about 36% & 53% at upstream side and downstream side of pier respectively in relative to their counterparts related to the circular cylinder.

As stated by [9], an experimental study have been conducted to assess the local scour around both of the vertical cylindrical pier and semi-conical piers and around both of the semi-conical pier and semi-conical piers which integrated with a number of devices as leading edge. Semi-conical piers have been subjected to a number of modifications to make their usage in the field applicable (Fig.1). Also, semi-conical piers with different small angles of side slope (2.86^0, 5.7^0 & 8.5^0), rectangular section, and constant base (D_2) are used. To improve the efficiency of modified semi-conical pier in reducing the local scour, a number of devices were incorporated with

the leading edge of this pier. All experiment have been run under condition of steady clear water with test duration of 4 hours. The results have shown that the maximum decrease (25% and 60% respectively) in depth and volume of scour are observed for semi-conical pier in relative to the cylindrical pier. Also, the maximum decrease (37.8 & 68% respectively) in the depth and volume of scour are observed for semi-conical pier with upstream curved face device (Fig.2) compared with the semi-conical pier without this device.

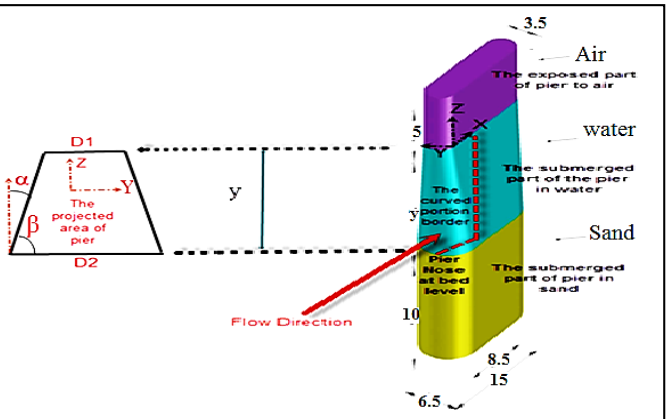

Fig. 1. The semi-conical pier.

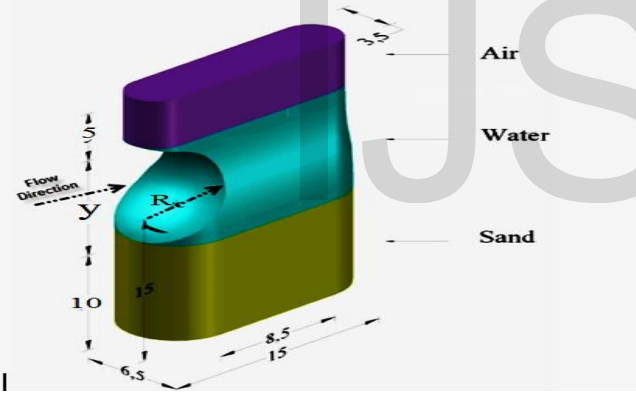

Fig. 2. The semi-conical pier with upstream curved face.

In Fig.1, D_1 and D_2 are the diameter of pier at water surface and bed level respectively. α and y are the side slope angle and the approach flow depth. In Fig.2, *Rc*, which suggested to equal to D_2-D_1, is the arc height of curvature and it is introduced as the horizontal distance which begins from the nose of pier to inside the body of pier. The curvature begins from water surface level to bed level.

In this paper, piers in Fig.1. & Fig.2. are taken into consideration to develop pier scour equations.

3 Experimental Set-up

All experiments have been run at a rectangular straight flume with dimension of 6.8m (length) × 0.74m (width) × 0.4m (height). This flume is located at the Hydraulic Laboratory, Department of Irrigation and Hydraulics, Engineering Faculty, University of Mansoura, Egypt. A rectangular weir, which placed at upstream of flume, has been used to measure the flow discharge. Furthermore, at the channel end, a tail gate is placed to control water depth. In addition, a mobile point gauge with an accuracy of ± 0.1mm has been used to measure the scour depth, bed levels, and water depth. Fig. 3 shows the experimental set-up.

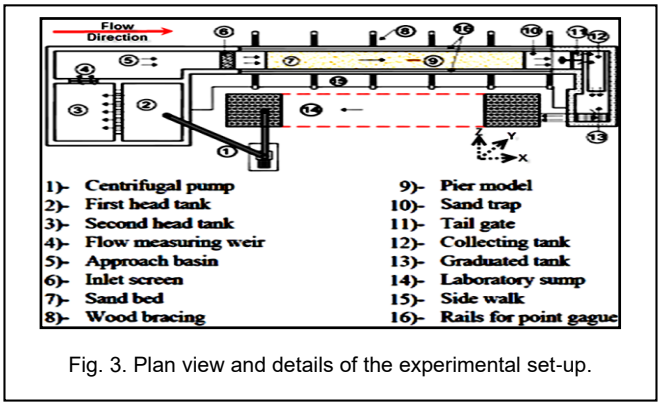

Fig. 3. Plan view and details of the experimental set-up.

4 Bed Material

Sand with 10 cm thickness has been spread along more than 90% of flume bed. Therefore, the width and length of tested section are 0.74 and 6.1 m respectively. Moreover, the sand 's characteristic properties are: the geometric standard deviation (σg) = 2 and the median size of particle (d_{50}) = 0.71 mm. So, the bed material is classified as the non-uniform due to σg>1.3 and armoring happens in the scour hole and on the bed of channel as mentioned by stated by Melville (1997), cited in [15].

5 Piers

All pier models are made of wood and they are painted with a glue material (varnish) to prevent a penetration of water when piers are used in the flume. Moreover, after sand leveling, piers have been mounted in the flume center with orientation 0.0 degree to the flow direction to prevent the influence of flume sidewalls and to attain the condition of fully developed flow. Dimensions of used piers are clarified in TABLE 1 & TABLE 2. It should be mentioned that the length (*L*) of semi-conical piers is selected depending on the ratio of (L/D=3), in which *D* is mean diameter equal to (D_1+D_2/2). As well, the lengths of semi-conical pier are not given in TABLE 1 & TABLE 2 because they have no influence on local scour since an attack angle for all experiments has been kept constant.

6 Lab Procedures

To achieve the aims of this paper, three depths of flow with their corresponding discharges are used. Also, all experiments subject to the condition of steady clear-water and test duration of 4 hours. According to [4] and [11], three or four hours can provide or show the maximum occurrence of local scour depth. This test duration has been proved during conducting the experimental work of this paper when the time development of scour depth is almost asymptotic at the end of 4h. Furthermore, because the used bed material is non-uniform, the formulas, which suggested by Melville and Coleman (2000),

cited in [7], are used to find the critical shear velocity and its corresponding critical velocity. These formulas are as follows:-

$$u_{*ca} = 0.0115 + 0.012\, d_{50a}^{1.4},\ 0.1\text{ mm} < d_{50a} < 1\text{ mm} \quad (1)$$

$$u_{*ca} = 0.0305\sqrt{d_{50a}} - \frac{0.0065}{d_{50a}},\ 1\text{ mm} < d_{50a} < 100\text{ mm} \quad (2)$$

$$\frac{V_{ca}}{u_{*ca}} = 5.75\,\mathrm{Log}\,(5.53\,\frac{y}{d_{50a}}) \quad (3)$$

$$V_a = 0.8\,V_{ca} \quad (4)$$

$$d_{50\,a} = \frac{d_{max}}{1.8} \quad (5)$$

In which:- V_a is the critical mean velocity and it is used to mark the transition from condition of clear-water to the condition of live-bed for non-uniform sediments transported by the flow, V_{ca} is mean velocity of approach flow beyond which the armoring of the non-uniform sediment bed is not possible, u_{*ca} is the critical shear velocity, d_{50a} is size of median armor, and d_{max} is size of maximum particle and it is obtained from the particle size distribution curve.

7 Theoretical Approach

To develop equations of pier scour, the dimensional analysis has been applied. As pointed out by [5], the local scour depth at the pier of bridge can be linked to some variables, which illustrated in Eq.(6), as its independent variables.

$$d_s = f_1\,[\text{Bed sediment}\,(V_c, \rho_s, \sigma_g, d_{50}), \text{Flood flow}\,(g, y, V, \nu, \rho), \text{Bridge geometry}\,(D, Sh_{Sh}, Al), \text{Time}\,(T)] \quad (6)$$

In which, d_s is the maximum depth of local scour; ρ and ν are the fluid density and the kinematic viscosity respectively; g is the gravity acceleration; y is the depth of approach flow; σg is the geometric standard deviation of the distribution of sediment particle size; d_{50} is the median size; V is the velocity of mean approach flow; V_c is the critical mean approach velocity for the bed sediment entrainment; ρ_s is the density of sediment; Al and Sh_{Sh} are parameters describing the pier alignment and the pier shape respectively; T is the time; D is the width of pier; and f_1 is "a function of".

Another independent variable is added to Eq.(6) to show its effect on the scour depth. This variable is the side slope angle (α). Previously, adding the angle to the independent variables of local scour depth has been adopted by researchers. For example, [10] has studied the influence of inclination angle on maximum local scour depth. The inclination angle is related to inclined circular piers. According to [14], the inclined circular pier is considered as alternative to semi-conical pier. Consequently, Eq.(6) can be re-written as follows:

$$d_s = f_2\,[V_c, \rho_s, \sigma_g, d_{50}, g, y, V, \nu, \rho, D, Sh_{Sh}, Al, T, \alpha] \quad (7)$$

The Buckingham's π theorem and the repeating variables (ρ, V, y) are used for Eq.(7) to obtain a new dimensionless functional relationship as follows:

$$\frac{d_s}{y} = f_3\left(\frac{V}{V_c}, \frac{V^2}{gy}, \frac{D}{y}, \frac{Vy}{\nu}, \frac{d_{50}}{y}, \frac{VT}{y}, \sigma_g, Sh_{Sh}, Al, \alpha, \frac{\rho_s}{\rho}\right) \quad (8)$$

Eq.(8), as well, can be rearranged to be:

$$\frac{d_s}{y} = f_4\left(\frac{V}{V_c}, \frac{V^2}{gy}, \frac{VT}{D}, \frac{Vd_{50}}{\nu}, \sigma_g, Sh_{Sh}, Al, \alpha, \frac{\rho_s}{\rho}\right) \quad (9)$$

Eq. (9) can be simplified if the following assumptions are adopted:

- (VT/D) can be ignored if the duration of flow is long enough and the depth of equilibrium scour is studied [10].
- For fully turbulent flow, the effect of Reynolds number is neglected. Hence, (Vd_{50}/ν), which is the particle Reynolds number, can be ignored [10].
- (σ_g) can be ignored if the properties of bed material are not changed [10].
- (ρ_s/ρ) can be ignored if densities of sediment and fluid are kept constant [5].
- Alignment factor (Al) can be ignored if the attack angle in all experiments is kept equal zero degree.
- In the present research, the shape factor (Sh_{Sh}) is ignored because the change in pier shapes is due to the change in the side slope angle and not due to use different pier shapes having similar perpendicular width relative to the flow direction.

After simplifying Eq.(9), the next equation can be considered:

$$\frac{d_s}{y} = f_5\left(\frac{V}{V_c}, \frac{V^2}{gy}, \alpha\right) \quad (10)$$

Due to the effect of armoring, (Vc) in Eq.(10) can be substituted by (Va). Also, the Froude number (V^2/gy) is expressed usually as $(V/(gy)^{0.5})$ [13]. So, Eq. (10) can be expressed as follows:

$$\frac{d_s}{y} = f_6\left(\frac{V}{V_a}, \frac{V}{\sqrt{gy}}, \alpha\right) \quad (11)$$

Another equation is derived to expect the depth of maximum normalized scour which resulted by semi-conical pier with curved face (illustrated in Fig.2). This equation is expressed as follows:

$$\frac{d_s}{y} = f_7\left(\frac{V}{V_a}, \frac{V}{\sqrt{gy}}, \frac{R_c}{y}\right) \quad (12)$$

In which R_c is Arc height of curvature as mentioned and shown previously in Fig.2.

8 Results and Discussion

8.1 The Semi-conical Piers

In the multiple regression analyses, β is used instead of α in Eq.(11) to avoid the zero degree angle as shown in TABLE 1. β is equal to 90^0 - α and it is inserted in radians. Therefore, Eq. (11) can be expressed as follows:

$$\frac{d_s}{y} = f_8\left(\frac{V}{V_a}, \frac{V}{\sqrt{gy}}, \beta\right) \quad \ldots\ldots(13)$$

In the present paper, the effect of flow intensity (V/V_a) and Froude number ($Fr = V/(gy)^{0.5}$) on (d_s/y) is examined separately with different side slope angle. This procedure has been previously adopted in previous studies, [14], and [15]. Therefore, two equations can be obtained from Eq.(13) as follows:

$$\frac{d_s}{y} = f_9\left(F_r, \beta\right) \quad \ldots\ldots(14)$$

$$\frac{d_s}{y} = f_{10}\left(\frac{V}{V_a}, \beta\right) \quad \ldots\ldots(15)$$

The following two equations are considered instead of Eq. (14 & 15) because they are a desired form for the experimental results which related to this paper.

$$\frac{d_s}{y} = C\,(F_r)^{C1}\,(\beta)^{C2} \quad \ldots\ldots(16)$$

$$\frac{d_s}{y} = C\,\left(\frac{V}{V_a}\right)^{C1}\,(\beta)^{C2} \quad \ldots\ldots(17)$$

C, C_1 & C_2 in Eq. (16) & Eq.(17) are constants and they are determined using multiple regression analysis. Therefore, Eq.(16 & 17) are expressed in a general form of equation of multiple regression (as illustrated in Eq. (18 & 19)).

$$\log\left(\frac{d_s}{y}\right) = \log C + C_1 \log\left(F_r\right) + C_2 \log\left(\beta\right) \quad \ldots\ldots(18)$$

$$\log\left(\frac{d_s}{y}\right) = \log C + C_1 \log\left(\frac{V}{V_a}\right) + C_2 \log(\beta) \quad \ldots\ldots(19)$$

After values of C, C_1 & C_2 are determined, the following two equations are obtained:

$$\frac{d_s}{y} = 14.2088\,(F_r)^{3.3970}\,(\beta)^{1.9551} \quad \ldots\ldots(20)$$

$$\frac{d_s}{y} = 0.4294\,\left(\frac{V}{V_a}\right)^{3.0534}\,(\beta)^{1.9551} \quad \ldots\ldots(21)$$

The aforementioned equations are developed using more than 65% of observations (dependent parameter, ds/y) and their corresponding independent parameters (V/Va ,Fr, β) that are revealed in TABLE 1.

It can be pointed out that there is a good agreement in Fig.(4&5) between the observed and estimated values of (ds/y) because most of these values closely converge on the line of perfect agreement ($R^2 = 1$).

TABLE 1
DIMENSIONAL VARIABLES AND DIMENSIONLESS PARAMETERS USED FOR DEVELOPING EQUATION 20 & 21.

Q Lit/s	Sym	α^0	β^0	D_2 cm	D_1 cm	D_{mean} cm	y cm	d_s cm	Dependent parameters ds/y	Independent parameters F_r	V/Va	β (rad)
17.023	Cy_2	0	90	6.5	6.5	6.5	9.5	3.05	0.321	0.251	0.675	1.571
17.023	A_2	2.86	87.14	6.5	5.55	6.025	9.5	2.77	0.292	0.251	0.675	1.521
17.023	B_2	5.71	84.29	6.5	4.6	5.55	9.5	2.56	0.269	0.251	0.675	1.471
17.023	C_2	8.53	81.47	6.5	3.65	5.07	9.5	2.44	0.257	0.251	0.675	1.422
17.023	D_2	10	80	6.5	3.15	4.82	9.5	2.23	0.235	0.251	0.675	1.396
21.106	Cy	0	90	6.5	6.5	6.5	10	6	0.600	0.288	0.788	1.571
21.106	A	2.86	87.14	6.5	5.5	6	10	4.9	0.490	0.288	0.788	1.521
21.106	B	5.71	84.29	6.5	4.5	5.5	10	4.7	0.470	0.288	0.788	1.471
21.106	C	8.53	81.47	6.5	3.5	5	10	4.5	0.450	0.288	0.788	1.422
21.106	D	10	80	6.5	2.9	4.74	10	3.91	0.391	0.288	0.788	1.396
26.596	Cy_1	0	90	6.5	6.5	6.5	10.5	8.94	0.851	0.337	0.938	1.571
26.596	A_1	2.86	87.14	6.5	5.45	5.98	10.5	7.89	0.751	0.337	0.938	1.521
26.596	B_1	5.71	84.29	6.5	4.4	5.45	10.5	7.77	0.740	0.337	0.938	1.471
26.596	C_1	8.53	81.47	6.5	3.35	4.93	10.5	7.45	0.710	0.337	0.938	1.422
26.596	D_1	10	80	6.5	2.8	4.65	10.5	7.1	0.676	0.337	0.938	1.396

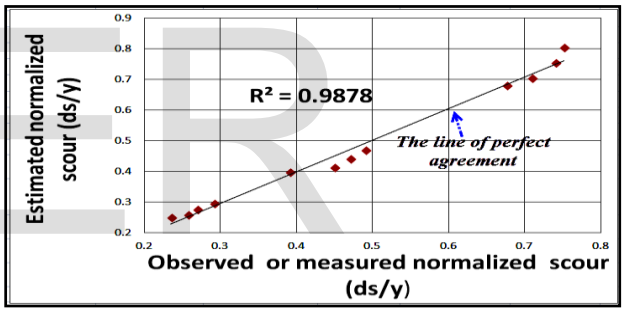

Fig. 4. The comparison between all the normalized measured (observed) scour (ds/y) and those estimated (computed) by proposed Eq. (20).

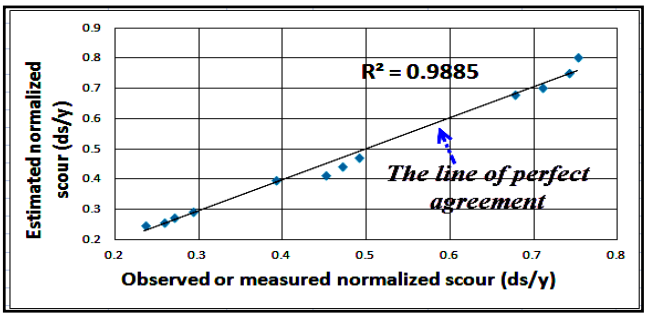

Fig. 5. The comparison between all the normalized measured (observed) scour (ds/y) and those estimated (computed) by proposed Eq. (21).

To check the precision of measurements, Eq.(20) & Eq.(21) are used for the remaining observations, particularly for their independent dimensionless parameters to estimate their val-

ues of (*ds/y*). After that, the estimated values of (*ds/y*) are compared with their observed values as shown in Fig.6 & Fig.7.

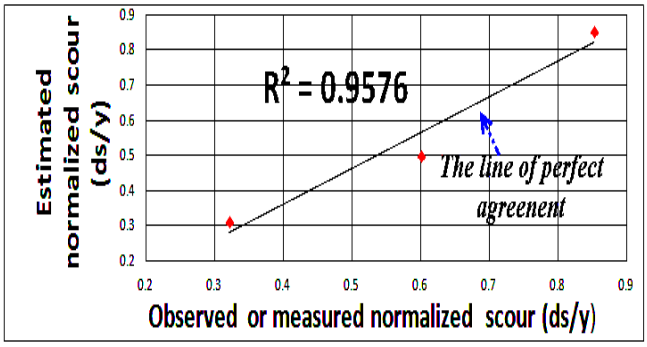

Fig. 6. The comparison between the normalized measured and estimated scour values of (ds/y) from Eq.(20) to check the validity of measurements.

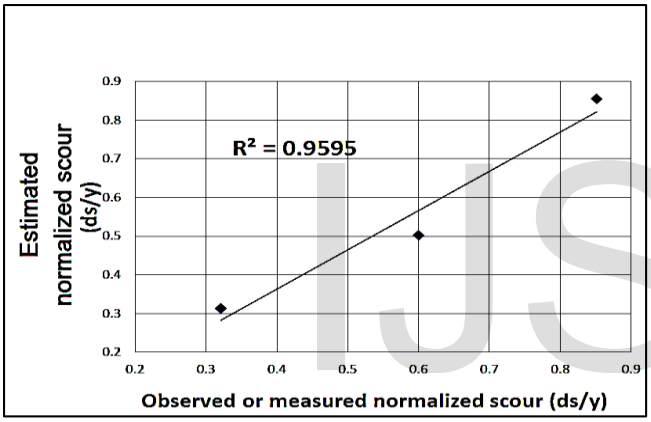

Fig. 7. The comparison between the normalized measured and estimated scour values of (ds/y) from Eq.(21) to check the validity of measurements.

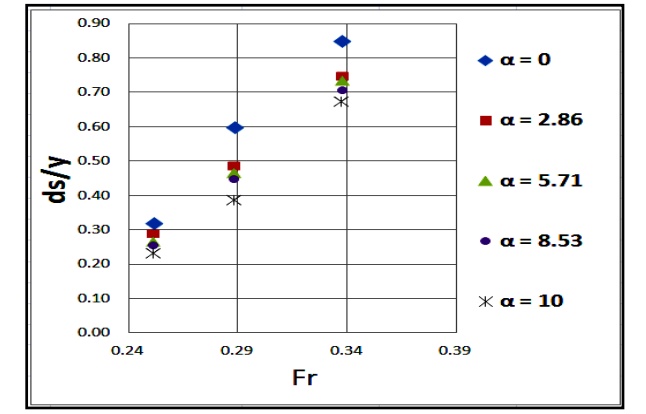

Fig. 8. The variations of (*ds/y*) with (*Fr*) for all the side slope angles.

or Fig (8 & 10), the normalized scour (*ds/y*) is directly proportional to the flow intensity (V/Va) & the Frude number (*Fr*).

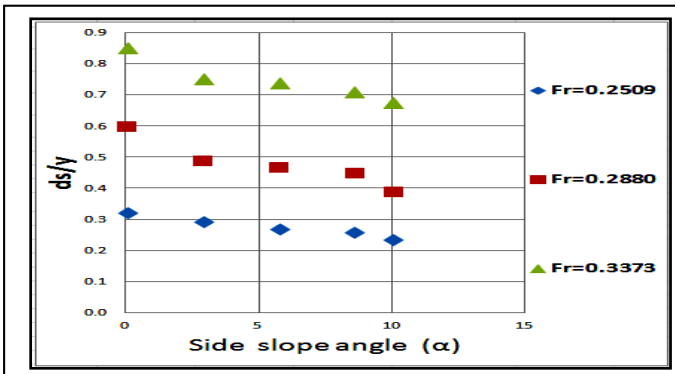

Fig. 9. The variation of (*ds/y*) with side slope angle for all Froude numbers.

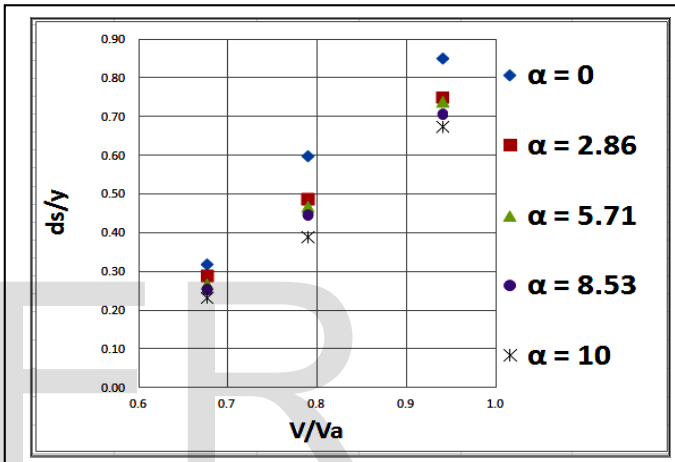

Fig. 10. The variation of (*ds/y*) with (*V/Va*) for all side slope angles.

For Fig(9), the normalized scour depth (*ds/y*) is inversely proportional to the side slope angle (α). So, increasing the angle of side slope leads to decrease normalized scour depth due to the reduction in the projected area of piers. According to [1], the scour depth at upstream pier is directly proportional to upstream projected area at nose of pier.

8.2 The Semi-conical pier with Curved Face

Eq.(12) subjects to the same previous assumption which adopted for Eq.(11). This assumption is to study the effect of each one (*V/Va, Fr*) separately with (*ds/y*). So, following two equations are obtained from Eq.(12):

$$\frac{d_s}{y} = f_{11}\left(\frac{V}{\sqrt{gy}}, \frac{R_c}{y}\right) \quad \ldots\ldots(22)$$

$$\frac{d_s}{y} = f_{12}\left(\frac{V}{V_a}, \frac{R_c}{y}\right) \quad \ldots\ldots(23)$$

To illustrate the final form for Eq.(22 & 23), multiple regression analysis and dependent parameter (d_s/y) and their corresponding independent parameters (V/Va,F_r, Rc/y) in TABLE 2 are employed:

$$\frac{d_s}{y} = 26.3675(F_r)^{3.6936}\left(\frac{R_c}{y}\right)^{-0.2003} \quad \ldots\ldots(24)$$

$$\frac{d_s}{y} = 0.5869\left(\frac{V}{V_a}\right)^{3.3186}\left(\frac{R_c}{y}\right)^{-0.2003} \quad \ldots\ldots(25)$$

Eq.(24 & 25) are developed using more than 65% of dependent parameters (*ds/y*) and their corresponding independent parameters (*V/Va, Fr, Rc/y*) illustrated in TABLE 2.

TABLE 2
DIMENSIONAL VARIABLES AND DIMENSIONLESS PARAMETERS USED FOR DEVELOPING EQUATIONS (24&25)

Q Lit/s	Sym	α^0	β^0	D_2 cm	D_1 cm	R_c cm	y cm	d_s cm	Dependent parameters ds/y	Independent parameters F_r	V/Va	R_c/y
17.023	E3A2	2.86	87.14	6.5	5.55	0.95	9.5	2.4	0.253	0.251	0.675	0.10
17.023	E3B2	5.71	84.29	6.5	4.6	1.90	9.5	2.1	0.221	0.251	0.675	0.20
17.023	E3C2	8.53	81.47	6.5	3.65	2.85	9.5	1.7	0.179	0.251	0.675	0.30
21.106	E3A	2.86	87.14	6.5	5.5	1.00	10	4.4	0.440	0.288	0.788	0.10
21.106	E3B	5.71	84.29	6.5	4.5	2.00	10	3.5	0.350	0.288	0.788	0.20
21.106	E3C	8.53	81.47	6.5	3.5	3.00	10	2.8	0.280	0.288	0.788	0.30
26.596	E3A1	2.86	87.14	6.5	5.45	1.05	10.5	7.6	0.724	0.337	0.938	0.10
26.596	E3B1	5.71	84.29	6.5	4.4	2.10	10.5	7.2	0.686	0.337	0.938	0.20
26.596	E3C2	8.53	81.47	6.5	3.35	3.15	10.5	6.8	0.648	0.337	0.938	0.30

It can be stated that there is the good agreement in Fig.(11&12) between the observed and estimated values of (*ds/y*) because most of these values closely converge on the line of perfect agreement ($R^2 = 1$).

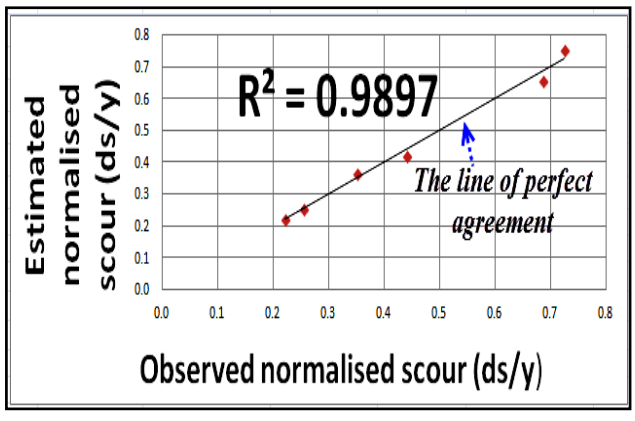

Fig. 11. The comparison between all the normalized measured (observed) scour (*ds/y*) and those estimated (computed) by proposed Eq. (24).

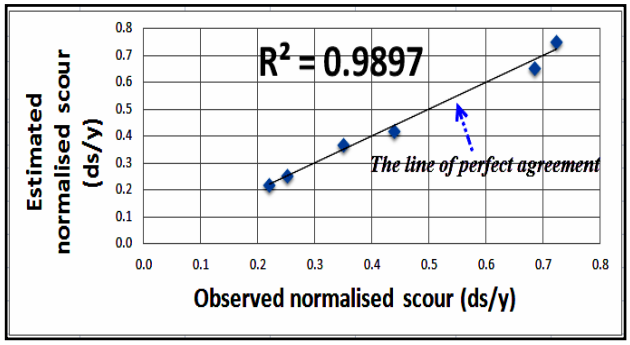

Fig. 12. The comparison between all the normalized measured (observed) scour (*ds/y*) and those estimated (computed) by proposed Eq. (25).

To check the precision of measurements,, Eq.(24) & Eq.(25) is used for the remaining observations, particularly for their independent dimensionless parameters to estimate their values of (*ds/y*). After that, the estimated values of (*ds/y*) are compared with their observed values (Fig.13 & Fig.14).

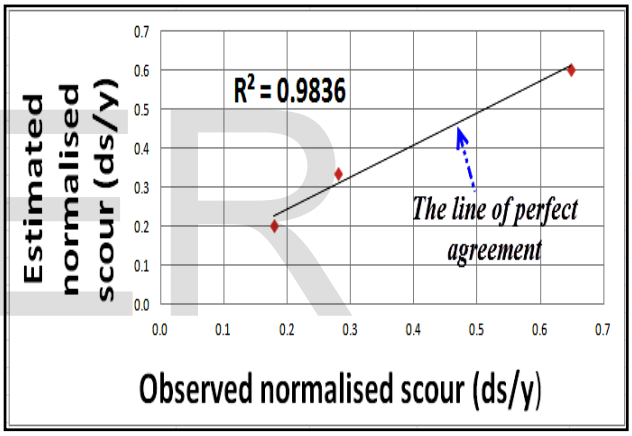

Fig. 13. The comparison between the normalized measured and estimated scour values of (ds/y) from Eq. 24 to check the validity of measurements

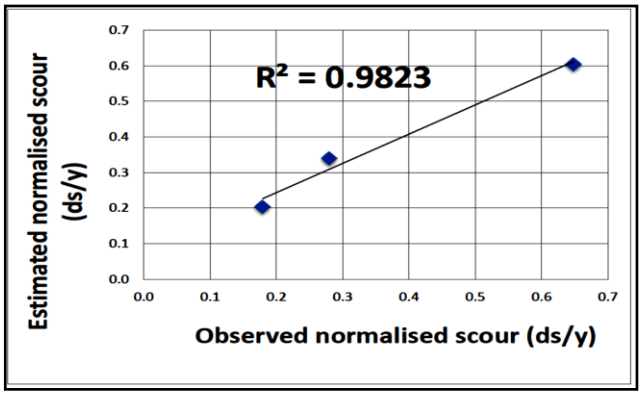

Fig. 14. The comparison between the normalized measured and estimated scour values of (ds/y) from Eq. 25 to check the validity of

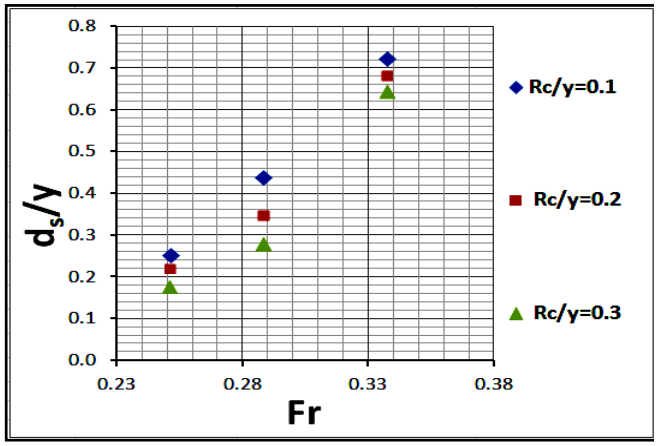

Fig. 15. The variations of (*ds/y*) with (*Fr*) for all Arc heights (*Rc/y*).

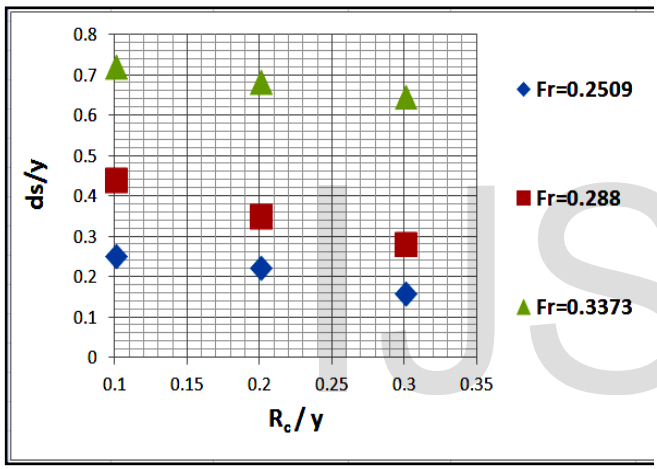

Fig. 16. The variations of (*ds/y*) with (*Fr*) for all Arc heights (*Rc/y*).

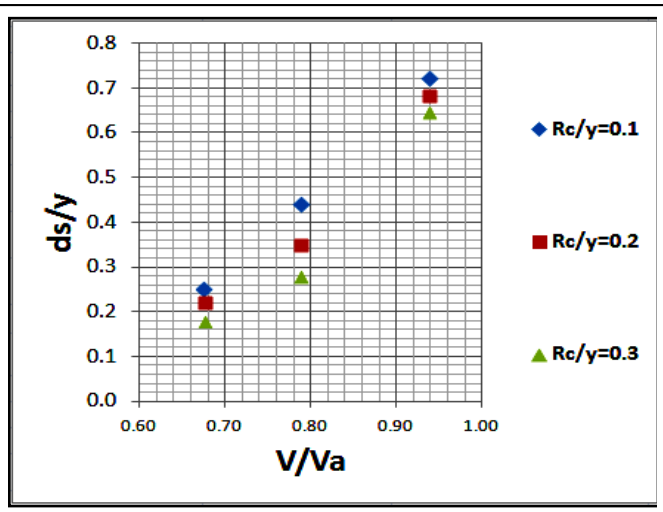

Fig. 17. The variations of (*ds/y*) with (*Va/V*) for all Arc heights (*Rc/y*).

For Fig (15 & 17), the normalized scour depth (*ds/y*) is directly proportional to the Frude number (*Fr*) & the flow intensity (V/Va)

For Fig(16), normalized Arc height of curved face is inversely proportional to the normalized scour (*ds/y*). So, increasing (*Rc/y*) leads to decrease (*ds/y*) because the curvature works to elongate the direction of downward flow or the approach flow direction to the pier nose, and then to orient it to be reversed to the direction of coming flow instead of impinging the material of bed nearby the pier nose. The elongation and orientation work to decrease a strength of the downward flow in impinging the bed material. As stated by Melville and Raudkivi (1977) cited in [12], the down flow or downward in literature is considered the main agent of scouring.

In the present paper, all experiments have been run at the condition of fully turbulent flow, so dropping (Vd_{50}/v) from Eq. (9) is justified. Also, all experiments have been subjected to test duration of 4 hours. Four hours are enough for the time development of scour depth to be almost asymptotic and to provide the equilibrium depth of scour. Hence, dropping *(VT/D)* from Eq.(9) is justified. As well, one bed material is used for all experiments, therefore dropping (σg, d_{50}, $\rho s/\rho$) from Eq.(9) are justified. Finally, the attack angle is kept to equal to zero degree, thus dropping *Al* from Eq.(9) is justified.

9 Conclusion

To ensure a safe design of bridge pier foundation, it is significant to develop equations that can guess accurately the maximum depth of scour at bridge piers. Consequently, scour equations at bridge piers are developed in this paper. These equations are related to modified semi-conical piers and modified semi-conical piers with curved face. Finally, the sort of relationship between the dependent and independent parameters of equations of this paper has been clarified to show the effect of independent parameters, namely the side slope angle, the Froude number, flow intensity, and normalized arc height of curve on the normalized depth of scour.

NOTATION

In this paper, the following symbols have been used:
α= Side slope angle of semi-conical pier (degree);
β= 90- α (degree)
σ_g= Geometric standard deviation;
D= Main diameter of pier (cm);
D_1 = Diameter of pier at the water surface level (cm);
D_2 = Diameter of pier at the bed level (cm);
D_{50} = Median particle size (mm);
D_{50a} =Median sediment size for the possible coarsest armor (mm);
d_{max}= Maximum particle size (mm);
d_s=Maximum scour depth around piers (cm);
y=Approach flow depth (cm);

L= Pier length (cm);
Q= Flow discharge (L/s);
V= Mean velocity (m/s);
V_a= Critical mean velocity (m/s) for non-uniform sediment;
V_{ca}= Mean velocity of approach flow beyond which the armoring of non-uniform bed is not possible;
V_c= Critical mean approach velocity (m/s) for uniform sediment;
Al & Sh_{sh} = Parameters describing the pier alignment and the pier shape, respectively;
T= Time (s);
ρ & ρ_s= Fluid and sediment densities;
g= Gravity acceleration;
υ= Kinematic viscosity;
u_{*ca}= Critical shear velocity;
R_c=Arc height.

REFERENCES

[1] A.-H.K. Al-shukur and Z.H. Obied, "Experimental study of bridge pier shape to minimize local scour," *International Journal of Civil Engineering and Technology,* vol. 7, no. 1, pp. 162-171, Jan-Feb. 2016.

[2] A. Ismael, M. Gunal and H. Hussein, "Influence of bridge pier position according to flow direction on scour reduction," *ACSEE*, pp. 12-16, 2013.

[3] A. Ismael, M. Gunal and H. Hussein, "Use of Downfoil-Shaped Bridge Piers to Reduce Local Scour," *Journal Impact Factor,* vol. 5, no. 11, pp. 44-56, Nov. 2014.

[4] A.M. Yanmaz and H.D. Altinblek, "Study of time –dependent local scour around bridge piers," *J. Hydraul. Eng.,* vol. 117, no. 10, pp. 1247-1268, Oct. 1991.

[5] B. Melville, "The Physics of Local Scour at Bridge Piers," *4thInt.Conf. on Scour and Erosion*, pp. 28-40, 2008.

[6] D.M. Drysdale, "The effectiveness of an aerofoil shaped pier in reducing downstream vortices and turbulence," BSc dissertation, Faculty of Engineering and Surveying, University of Southern Queensland, 2008.

[7] D.Roy and M.A Matin, "An assessment of local scour at flood-plain and main channel of compound channel section.," *Journal of Civil Engineering,* vol. 38, no. 1, pp. 39-52, 2010.

[8] H. Hakimzadeh, R. Mehrzad and N. Azari, "Experimental investigation of the effects of slotted coni-cal shaped Piers on scour process due to steady flow," *ICSE6 Paris*, pp.189-195, available at http://scour-and-erosion.baw.de/icse6-cd/data/articles/000272.pdf , Aug. 2012.

[9] K.S. El-Alfy, M.T. Shamaa and H.H. Al-tameemi, "Reducing the local Scour around Bridge Piers by Using Semi-conical Piers," *Mansoura Engineering Journal,* vol. 42, no. 2, pp. 10-19, June 2017.

[10] M.C. Ozalp, "Experimental Investigation of Local Scour Around Bridge Pier Groups," MSc Dissertation, Dept. of Civil Engineering, Middle East Technical University, 2013.

[11] M.d. Mia and H. Nago, "Design method of time dependent local scour at a circular bridge pier," Journal Hydraulic Engineering, vol. 129, no. 6, pp. 420-427, May 2003.

[12] P.D. Alabi, "Time Development of Local Scour at A Bridge Pier Fitted with A Collar," MSc dissertation, Dept. of Civil and Geological Eng., Saskatchewan University, 2006.

[13] R.E. Featherstone and C. Nalluri, *Civil engineering hydraulics*. Blackwell Science, USA.

[14] Z. Bozkus and O. Yildiz, "Effects of inclination of bridge piers on scouring depth," *Journal of Hydraulic Engineering,* vol. 130, no. 8, pp. 827-832, Aug. 2004.

[15] Z. Bozkus and M. Cesme, "Reduction of scouring depth by using inclined piers," *J. Civ. Eng.*, vol. 37, pp. 1621-1630, available at http://users.metu.edu.tr/bozkus/html/Reduction%20of%20scouring%20depth%20by%20using%20inclined%20piers.pdf, Oct. 2010.

[16] Y. Aghaee-Shalmani and H. Hakimzadeh, "Experimental investigation of scour around semi-conical piers under steady current action," *European Journal of Environmental and Civil Engineering*, vol.19, no.6, pp. pp. 717–732, Oct. 2014.